2013 IEEE/RSJ International Conference on
Intelligent Robots and Systems (IROS)
November 3-7, 2013. Tokyo, Japan

Development of Microhand Utilizing Singularity of Parallel Mechanism

Toru Ejima[1], Kenichi Ohara[2], Masaru Kojima[1], Mitsuhiro Horade[1]
Tamio Tanikawa[3], Yasushi Mae[1], and Tatsuo Arai[1]

***Abstract*— In the fields of medicine and biology, it is essential to realize fine manipulation. Therefore, micromanipulation techniques and micromanipulators such as microgrippers and optical tweezers have been developed. We have developed a two-fingered microhand which is using the parallel mechanism to realize precise and stable micromanipulation. However, the previous microhand has problems about workspace and vibration. In this paper, the development of a new microhand which solves problems of previous microhand. The characteristic of new microhand is to enlarge the workspace utilizing the singularity of the parallel mechanisms. Inverse kinematics and structural analysis are used to analyze the workspace, and we show that results of two analyses match. Vibration analysis simulates transportation task and grasping task for manipulation. The new microhand has a potential to reduce the vibration by vibration analysis results.**

***Index Terms*— Two-Fingered Microhand, Parallel Mechanism, Singularity**

I. Introduction

In the fields of medicine and biology, researches on tissue engineering are conducted extensively. Manipulation of micro-objects while observing them under a microscope is one of the frequently tasks in these researches, and its importance led to the introduction of assisted micromanipulation with micro-robotics systems such as an optical tweezer[1], a microgripper[2], and a microfluidic chip[3]. Micromanipulation requires precise and stable positioning. We have solved this problem by developing a two-fingered microhand.

The two-fingered microhand has a structure which imitates the use of chopsticks[4], the system summary[5] is shown in Fig. 1. A transportation task on the system is realized by stages of the lower module, and grasping task is realized by the parallel mechanism of the upper module. Parallel mechanism, which is used in two-fingered microhand system, has many advantage for micromanipulation such as precise positioning and high stiffness. As the reasons, many researchers have studied parallel mechanisms which have link mechanisms placed at even intervals. However, the size of previous parallel mechanisms is generally larger than the size of the general microhand, these parallel mechanisms can use various joints. Therefore, it is important to realize compact joints and to combine them when applying parallel mechanisms to the microhand. Piezoelectric elements which are used as actuators in a previous microhand model[6] have high responsibility and resolution. However, the maximum motion range of piezoelectric actuators is approximately a thousand of the length of a piezoelectric actuator. For realizing a microhand which has a large workspace, piezoelectric actuators should be appropriately used with consideration to their structure. As the previous microhand is developed after consideration of above-mentioned points, it does not work as well in the real workspace as in the simulated workspace. Furthermore, the previous microhand drops a grasping object at high-speed micromanipulation, because of low stiffness in the part of structure.

In this paper, we discuss design guidelines for a new mi-

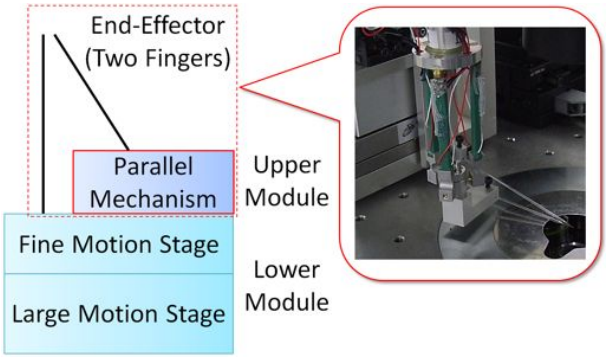

Fig. 1. Two-Fingered microhand system.

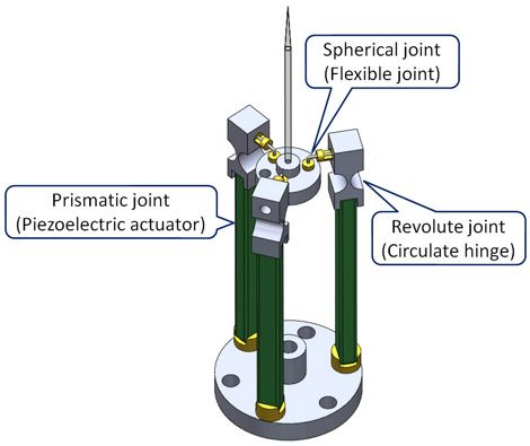

Fig. 2. CAD image of the 3-PRS model.

This work was supported by Grant-in-Aid for Scientific Research on Innovative Areas "Bio Assembler" (23106005) from the Ministry of Education, Culture, Sports, Science and Technology of Japan.

[1]T. Ejima, M. Kojima, M. Horade, Y. Mae, and T. Arai are with the Department of Systems Innovation, Osaka University, 1-3, Machikaneyama, Toyonaka, Osaka, 560-8531, Japan.

[2]K. Ohara is with the Faculty of Science and Technology, Meijo University, 1-501, Shiogamaguchi, Tenpaku, Nagoya, Aichi, 468-8502, Japan.kohara@meijo-u.ac.jp

[3]T. Tanikawa is with the Intelligenet Systems Research Institute, National Institute of Advanced Industrial Science and Technology, 1-1-1, Umezono, Tsukuba, Ibaraki, 305-8568, Japan.

crohand to solve above problems, and propose a microhand which has a large workspace by utilizing the singularity of the parallel mechanisms.

II. Design Concept of New Microhand Structure

A. Problem Analysis of a 3-PRS Parallel Mechanism

In Fig. 2, the microhand developed by A. Ramadan et al.[6] has a 3-Prismatic Revolute Spherical (3-PRS) parallel mechanism. The 3-PRS parallel mechanism is composed of 3 serial link mechanisms with prismatic revolute spherical joints from the base plate to the end-effector. Piezoelectric actuators are used as prismatic joints. A flexure hinge is used as a revolute joint. A flexible joint is used as a spherical joint, and contains a thin wire which facilitates bending and twisting. The 3-PRS parallel mechanism has one transitional DOF and two rotational DOFs.

The 3-PRS parallel mechanism has three critical problems as shown in below. Firstly, the 3-PRS parallel mechanism does not utilize the two rotational DOFs. The two rotational DOFs affect the workspace of horizontal direction because these DOFs can swing the end-effector in the same direction. This shows that the workspace is enlarged when expanding displacement for the vertical direction is realized. However, the displacement for the vertical direction in the 3-PRS parallel mechanism depends on the extension of the piezoelectric actuator because the piezoelectric actuators are placed parallel to the vertical direction. Secondly, the 3-PRS parallel mechanism does not work as well in the real workspace as in the simulated workspace because stiffness of the flexible joint is much lower than one of the flexure hinge. Furthermore, it is difficult to produce the flexible joint because of very compact and complicated structure. Finally, the end-effector with the 3-PRS parallel mechanism vibrates widely[7] because a part of 3-PRS parallel mechanism does not satisfy required stiffness for stable micro manipulation in high speed movement. The low stiffness problem should be solved, and the main causes of the problem are the flexible joints and the fabrication procedure such as a distortion of the bonding plane at the piezoelectric actuators.

B. Design Guideline for a New Microhand

Based on the problem analysis for previous microhand structure, we set the design guideline as shown in below:

1) 3-DOFs with one transitional DOF and two rotational DOFs.
2) Piezoelectric actuator used in a prismatic joint.
3) Flexure hinge used as a revolute joint.
4) Enlarging the displacement in the Z-axial direction by the singularity of the parallel mechanism.
5) Only using revolute joints as passive joints
6) Configure a prismatic joint by a piezoelectric actuator and a prismatic mechanism[8]

1), 2) and 3) refer to the advantage of the 3-PRS parallel mechanism. 4) is an important specification for enlarging the workspace by the singularity of the parallel mechanism[9],[10]. As far as 5) concerned, we consider that the new microhand should consist of same-stiffness passive joints to solve the workspace problem and the stiffness problem. 6) is achieved high stiffness because the piezoelectric actuator is embedded the prismatic mechanism and the bonding process of the piezoelectric actuators in the 3-PRS parallel mechanism, which is one of the cause of error, is eliminated. Furthermore, the prismatic mechanism compensates straight-running of the piezoelectric actuator.

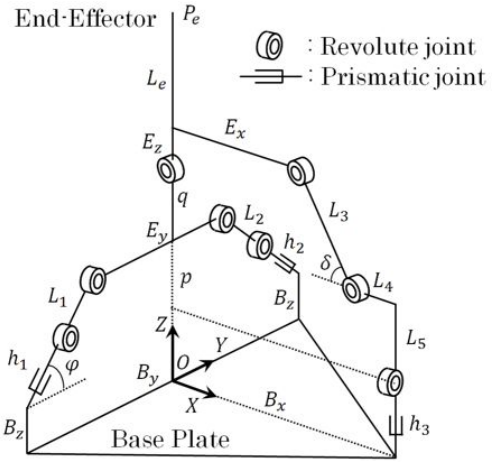

Fig. 3. Proposed model.

C. Proposed model for a New Microhand

A proposed model is shown in Fig. 3. The basic structure of the proposed model refers a mechanism proposed by J. Nielsen et al[11]. This microhand has a planar parallel mechanism in the YZ plane. The main characteristic of the proposed model is that is applied the design guideline 4) to the planar parallel mechanism in the YZ plane. The method of enlarging the workspace by the singularity of the parallel mechanism is described briefly, the upward force on prismatic joints h_1 and h_2 are converted into vertical motion by giving the angle φ fabricated the prismatic mechanisms.

III. Workspace Analysis

To analyze the workspace of the proposed model, inverse kinematics and structural analysis are applied. In inverse kinematics, the revolute joints of the proposed model are ideal joints excluding stiffness and force. However, the flexure hinge used as the revolute joint should be considered stiffness and force. Therefore, we use structural analysis to solve the problem that the 3-PRS parallel mechanism does not work as well in the real workspace as in the simulated workspace by inverse kinematics. Structural analysis finds out stress concentration of passive joints and displacement of the end-effector.

A. Inverse Kinematics

For the proposed model, the inverse kinematics problem can be stated as follows: for a given location of the end-effector $P_e(P_{ex}, P_{ey}, P_{ez})$, find the piezoelectric actuators parameters h_1, h_2, and h_3. The solution to the inverse kinematics problem is indicated below.

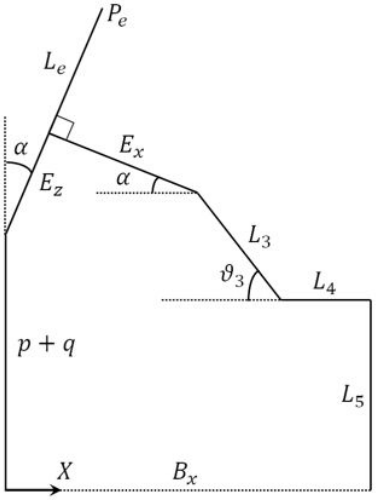

Fig. 4. The mechanism of the proposed model in the plane defined by p and the axis of the revolute joint at L_5.

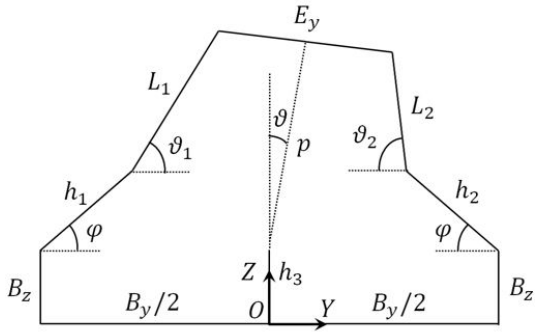

Fig. 5. The linkage alignment of the proposed model on the YZ plane.

The proposed model in the plane defined by p and the axis of the revolute joint at L_5 is shown in Fig. 4. The linkage alignment of the proposed model on the YZ plane is shown in Fig. 5. The component of the end-effector is given in Figs. 4 and 5:

$$P_{ex} = (E_z + L_e)\sin\alpha \quad (1)$$

$$P_{ey} = \{p + q + (E_z + L_e)\cos\alpha\}\sin\theta \quad (2)$$

$$P_{ez} = h_3 + \{p + q + (E_z + L_e)\cos\alpha\}\cos\theta \quad (3)$$

In this equation, we set the assumption that L_e is a extension of E_z. The equation is expressed below based on Fig.4:

$$E_z\sin\alpha + E_x\cos\alpha + L_3\cos\theta_3 + L_4 = B_x \quad (4)$$

$$p + q + E_z\cos\alpha = E_x\sin\alpha + L_3\sin\theta_3 + L_5 \quad (5)$$

To solve h_3, we focus on Eq.(1)-(5). The angle α is calculated by Eq.(1), and the angle θ_3 is calculated by substituting α into Eq.(4). Then, the unknown parameter p is calculated by Eq.(5), and the angle θ_3 is calculated by Eq.(2). Therefore, it is now possible to find the values of h_3 in terms of P_e by substituting the above parameters into Eq.(3).

Next, to solve remaining h_1 and h_2, we focus on two polygons separated by the boundary of p in Fig.5. Eq.(6) and (7) expressed the equation of each axial direction in the left polygon. Similarly, Eq.(8) and (9) is expressed by the right polygon.

$$h_1\cos\varphi + L_1\cos\theta_1 + \frac{E_y}{2}\cos\theta = \frac{B_y}{2} + p\sin\theta \quad (6)$$

$$B_z + h_1\sin\varphi + L_1\sin\theta_1 = h_3 + p\cos\theta + \frac{E_y}{2}\sin\theta \quad (7)$$

$$h_2\cos\varphi + L_2\cos\theta_2 + \frac{E_y}{2}\cos\theta + p\sin\theta = \frac{B_y}{2} \quad (8)$$

$$B_z + h_2\sin\varphi + L_2\sin\theta_2 + \frac{E_y}{2}\sin\theta = h_3 + p\cos\theta \quad (9)$$

To solve h_1 and h_2, the unknown angles θ_1 and θ_2 need to be found. The configurations of interest are given by:

$$\theta_i = \sin^{-1}\left(\frac{A_i\cos\varphi + B_i\sin\varphi}{L_i}\right) + \varphi \quad (i = 1, 2) \quad (10)$$

$$A_1 = h_3 + p\cos\theta + \frac{E_y}{2}\sin\theta - B_z \quad (11)$$

$$B_1 = \frac{E_y}{2}\cos\theta - \frac{B_y}{2} - p\sin\theta \quad (12)$$

$$A_2 = h_3 + p\cos\theta - \frac{E_y}{2}\sin\theta - B_z \quad (13)$$

$$B_2 = \frac{E_y}{2}\cos\theta - \frac{B_y}{2} + p\sin\theta \quad (14)$$

Therefore, it is now possible to find the values of h_1 and h_2 in terms of P_e by using Eq.(6) and (8). With all of the above results, we find the piezoelectric actuators parameters h_1, h_2, and h_3 in the proposed model.

B. Structural Analysis

To analyze the stress concentration and the workspace of the end-effector by ANSYS, the 3D design drawing of the proposed model is designed. We aim to downsize flexure hinges and shorten links because the 3-PRS parallel mechanism are not concentrated stress on passive joints. Furthermore, to improve stress concentration, the number of parts is reduced by composed some revolute joints of one part. The structural analysis can be stated as follows: for given the piezoelectric actuators parameters h_1, h_2, and h_3, find a displacement of the end-effector P_e and stress concentration.

The result of the deformation is shown in Fig.6, and the result of the stress concentration is shown in Fig.7. We

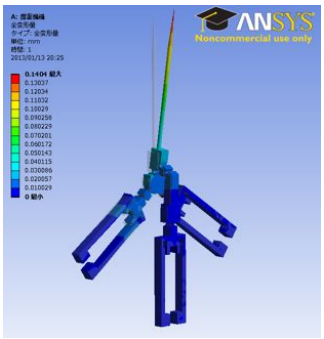

Fig. 6. The structural analysis result of the deformation.

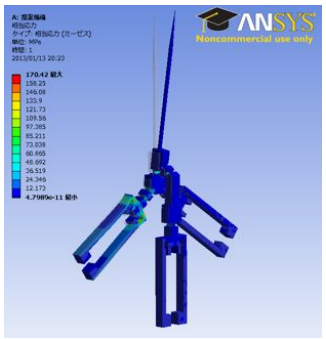

Fig. 7. The structural analysis result of the stress.

TABLE I

DESIGNED PARAMETER OF THE PROPOSED MODEL.

	E_x	E_y	E_z	q
$[mm]$	2.28	5.57	1.37	4.76
	$L_{1,2,3}$	L_4	L_5	L_e
$[mm]$	2.50	1.11	12.3	40.0

TABLE II

EACH AXIAL DISPLACEMENT OF WORKSPACE FOR THE PROPOSED MODEL BY TWO ANALYSES.

$[\mu m]$	Inverse kinematics	Structural analysis
X	-142 - 251	-154 - 251
Y	-61.0 - 61.0	-60.9 - 61.5
Z	0 - 29.8	0 - 28.0

give a $17.4\mu m$ displacement to the surface because it is the maximum extension of the piezoelectric actuators, which are used in the developed microhand. This result shows that the flexure hinges concentrate the stress and realize the intended motion.

C. Workspace Analysis Result

Design parameters agreed with two results of the inverse kinematics and the structural analysis are shown in TABLE I. In Fig.8, the result of the inverse kinematics is shown as blue plots, and the result of the structural analysis is shown as red lines. TABLE II shows the axial displacement of the workspace. Based on the above results we can say that, the proposed model is realized enlarging the workspace by using the singularity of the parallel mechanism, because the Z-axial displacement of the proposed model is larger than the maximum extension of the piezoelectric actuators $17.4\mu m$. Furthermore, the X-axial displacement of the proposed model is enough to realize manipulation tasks for a microobject. In Fig.9, a prototype of the proposed model using the parameters of TABLE I is designed.

IV. VIBRATION ANALYSIS

To verify the stiffness of the prototype of the proposed model, vibration analysis is applied to the prototype of the proposed model and the 3-PRS parallel mechanism by ANSYS. We simulated transportation task and grasping task on micromanipulation.

A. Simulation of Transportation Task

The transportation task on micromanipulation is realized by the motorized stages of the lower module in Fig.1. Therefore, if the prototype of the proposed model and the 3-PRS parallel mechanism were moved in the simulation, the vibration of the end-effector of each mechanism can be observed and compared. The result of simulation of transportation task for the 3-PRS parallel mechanism and the proposed model are shown in Fig.10 and 11, respectively. In TABLE III, maximum amplitudes and settling time is shown as evaluations of the stiffness. The settling time is defined as when the vibration amplitude is within $\pm 0.1\mu m$. With the above results, the prototype of the proposed model vibrates

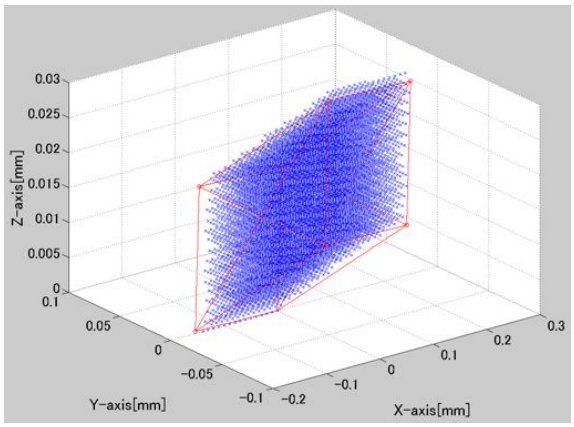

Fig. 8. Comparison of inverse kinematics result with structural analysis result for the proposed model.

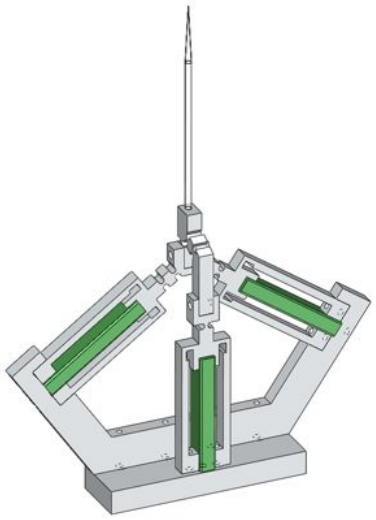

Fig. 9. CAD image of the proposed model for prototype fabrication.

much lower than the 3-PRS parallel mechanism. Therefore, the stiffness of the proposed model is higher than the stiffness of the 3-PRS parallel mechanism in the transportation task.

B. Grasping Task Simulation

The grasping task on micromanipulation is realized by driven the piezoelectric actuators of the microhand. As simulation input, a step response is applied only the extension of the piezoelectric actuator to the contact surface of the piezoelectric actuator and the prismatic mechanism. The responsivity of the piezoelectric actuator depends on the length of the piezoelectric actuator. The piezoelectric actuators in the 3-PRS parallel mechanism are $40mm$ in lengh. On the other hand, in the proposed model they are $20mm$ in length. Therefore, we give the responsivity of each length as simulation input. The result of the grasping task simulation for the 3-PRS parallel mechanism and the proposed model are shown in Fig.12 and 13. In TABLE IV, damping constants and settling time is shown as evaluations of the stiffness. The settling time is defined as when the vibration amplitude is within $\pm 1\mu m$. The damping constant

TABLE III

VIBRATION ANALYSIS RESULT OF SIMULATED TRANSPORTATION TASK FOR EACH MODEL.

Model	Amplitude$[\mu m]$	Settling time$[ms]$
3-PRS model	4.64	249
Proposed model	0.458	21.6

TABLE IV

VIBRATION ANALYSIS RESULT OF SIMULATED GRASPING TASK FOR EACH MODEL.

Model	Damping constant	Settling time$[ms]$
3-PRS model	0.0369	36.4
Proposed model	0.0415	21.8

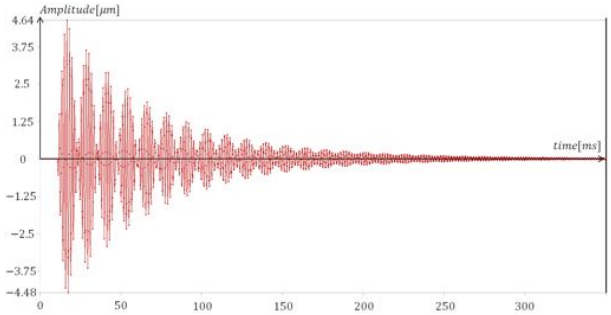

Fig. 10. Vibration analysis result of simulated transportation task for the 3-PRS model.

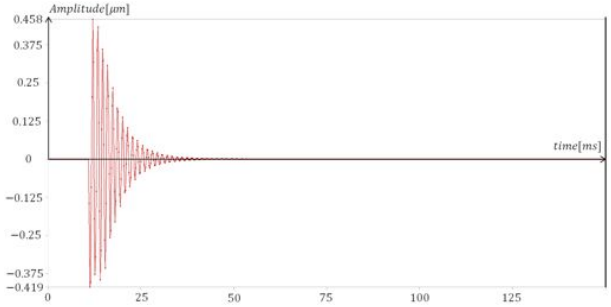

Fig. 11. Vibration analysis result of simulated transportation task for the proposed model.

is found using Eqs. (15) and (16):

$$h = \frac{\delta}{2\pi} \tag{15}$$

$$\delta = \frac{1}{m} \ln \frac{a_n}{a_{n+m}} \tag{16}$$

The parameter δ is the logarithm damping rate. The amplitude value after n periods is expressed a_n.

With the above results, the damping constant of the proposed model is larger than the damping constant of the 3-PRS parallel mechanism. Furthermore, the settling time of the proposed model is shorter than the settling time of the 3-PRS parallel mechanism. Therefore, the stiffness of the proposed model is higher than the stiffness of the 3-PRS parallel mechanism in the grasping task.

V. FABRICATION AND EXPERIMENT

In Fig.14, we fabricated the prototype of the proposed model based on the above analysis results. The prototype is

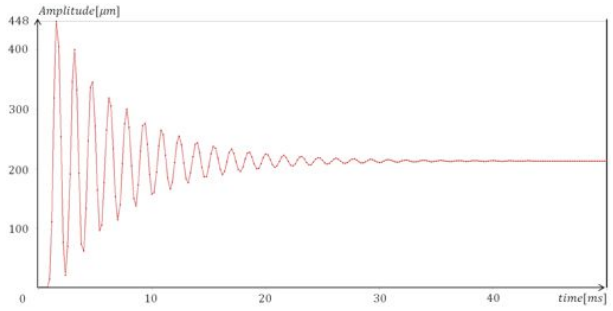

Fig. 12. Vibration analysis result of simulated grasping task for the 3-PRS model.

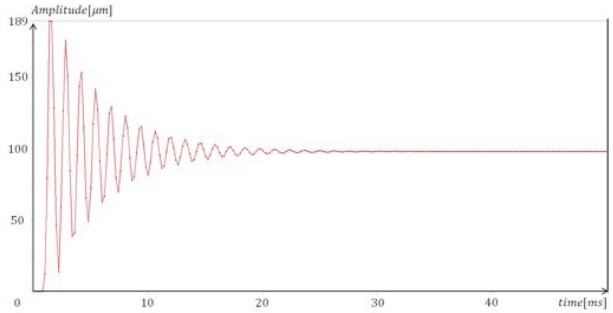

Fig. 13. Vibration analysis result of simulated grasping task for the proposed model.

used as the material of stainless steel because high stiffness is required. Each part of the prototype is fastened by screws and nuts. To compare real workspace of the prototype to the simulation result, the extensions of the piezoelectric actuators is measured by a microscope. As the piezoelectric actuators can extend $17.4\mu m$ in the specification, each actual extension of the piezoelectric actuators is $10.7\mu m$. The problem is considered that the stainless steel as the material has high stiffness.

We conduct experiments to measure a real workspace of the prototype. Displacements for each axial direction of the end-effector are measured in the case that each piezoelectric actuator is driven singularly. One example of the experimental result is shown in Fig. 15. In Fig. 15, the real workspace of the prototype is shown red lines, and the results of the inverse kinematics is shown blue plots in same condition of the prototype. In this experiment, the length of the end-effector L_e is $55mm$, and the maximum extension of the piezoelectric actuators is $10.7\mu m$ in the inverse kinematics. TABLE V shows the axial displacement of the workspace. The Y and positive X-axial displacement of the prototype are smaller than the result of the inverse kinematics, because small fastening powers and cutting errors of the electrical spark machining in fastening points decrease the workspace of the prototype. On the other hand, the Z and negative X-axial displacement are similar in the inverse kinematics. Given the actual extension of the piezoelectric actuators, the enlarging the Z-axial displacement by utilizing the singularity of the parallel mechanism is realized.

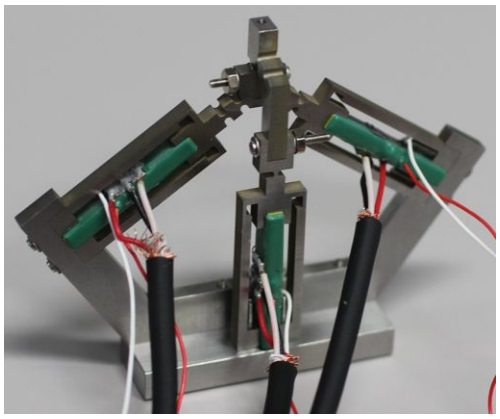

Fig. 14. Prototype of the proposed model.

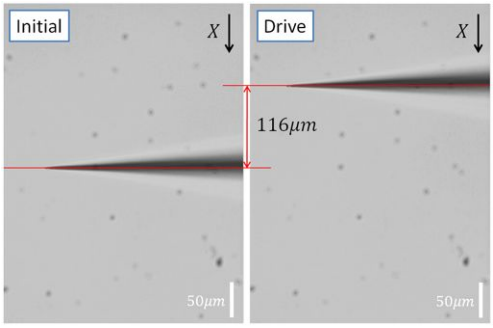

Fig. 15. Experiment for X axis in the case that h_3 is driven.

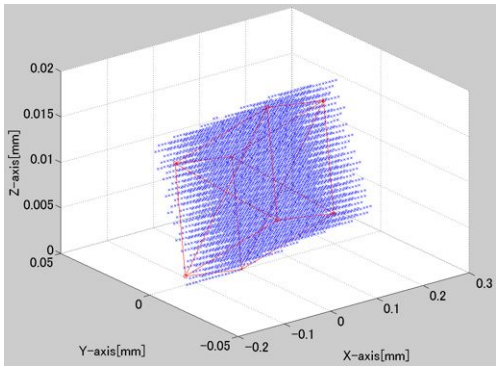

Fig. 16. Workspace result of the prototype.

VI. Conclusion

In this paper, we reported the developmental process of the new microhand which utilizes the singularity of the parallel mechanism. Firstly, we pointed out the problems of the previous microhand and then established design guidelines of for the new microhand. Secondly, a new model of microhand was proposed. Thirdly, the inverse kinematics and the structural analysis are applied to analyze the workspace of the proposed model because we maintain a consistency between the ideal revolute joints of the model and the actual flexure hinges. The two analysis results of the proposed model were same. Fourthly, we designed the prototype of the proposed model by 3D CAD and fabricated. Fifthly, the vibration analysis result showed that the proposed microhand is higher stiffness than the previous microhand. Finally, the workspace of the prototype was analyzed. The real workspace result showed that the proposed microhand realized the enlarging the workspace by utilizing the singularity of the parallel mechanism. Through the severel simulations and experiments, it can be said that the proposed microhand can realize stable and flexible operation compared with previous micro hand.

TABLE V

Each axial displacement of workspace for the prototype.

$[\mu m]$	Inverse kinematics	Experiment
X	-119 - 211	-116 - 148
Y	-48.2 - 48.2	-35.8 - 31.1
Z	0 - 18.4	0 - 18.2

As future works, we need to make an experiment of micromanipulation on the prototype. Furthermore, to verify the stiffness of prototype, we observe the vibration of the end-effector of the prototype with high speed micromanipulation.

References

[1] Hisataka Maruyama, Ryo Iitsuka, Kazuhisa Onda, Fumihito Arai: "Massive Parallel Assembly of Microbeads for Fabrication of Microtools Having Spherical Structure and Powerful Laser Manipulation," Proceedings of IEEE International Conference on Robotics and Automation, pp.482-487, 2010.

[2] Brandon K. Chen, Yong Zhang, Yu Sun: "Active Release of Microobjects Using a MEMS Microgripper to Overcome Adhesion Forces," Journal of Microelectromechanical Systems, Vol.18, No.3, 2009.

[3] Yoko Yamanishi, Shinya Sakuma, Tomohiro Iyanagi, Fumihito Arai, Tatsuo Arai, Akiyuki Hasegawa, Tamio Tanikawa, Akihiko Ichikawa, Osamu Satoh, Akihiro Nakayama, Hiroshi Aso, Mitsuhiro Goto, Seiya Takahashi, Kazutsugu Matsukawa: "Design and Fabrication of All-in-One Unified Microfluidic Chip for Automation of Embryonic Cell Manipulation," Journal of Robotics and Mechatronics, Vol.22, No.3, pp.371-379, 2010.

[4] Tamio Taikawa, Tatsuo Arai:"Development of a Micro-Manipulation System Having a Two-Fingered Micro-Hand," IEEE Transactions on Robotics and Automation, Vol.15, No.1, pp.152-162, 1999.

[5] Ebubekir Avci, Kenichi Ohara, Tomohito Takubo, Yasushi Mae, Tatsuo Arai: "A New Multi-Scale Micromanipulation System with Dexterous Motion", Proceedings of the 2009 International Symposium on Micro-Nano Mechatronics and Human Science, pp.444-449, 2009.

[6] Ahmed A.Ramadan, Tomohito Takubo, Yasushi Mae, Kenichi Oohara, and Tatsuo Arai: "Developmental Process of a Chopstick-Like Hybrid-Structure Two-Fingered Micromanipulator Hand for 3-D Manipulation of Microscopic Objects," IEEE Transactions on Industrial Electronics, Vol.56, No.4, pp.1121-1135, 2009.

[7] Ebubekir Avci, Chanh-Nghiem Nguyen, Christoph Gobel, Kenichi Ohara, Yasushi Mae, and Tatsuo Arai: "Vibration Analysis of Microhand for High Speed Single Cell Manipulation," Proceedings of 2012 IEEE International Conference on Mechatronics and Automation, pp.75-80, 2012.

[8] Qingsong Xu, Yangmin Li:"Mechanical Design of Compliant Parallel Micromanipulators for Nano Scale Manipulation," Proceedings of the 1st IEEE International Conference on Nano/Micro Engineered and Molecular Systems, pp.653-657, 2006.

[9] Robert Stoughton, and Tatsuo Arai:"Kinematic Optimization of a Chopstick-Type Micromanipulator," Proceedings of the Japan U.S.A Symposium on Flexible Automation, pp.151-157, 1992.

[10] Toru EJIMA, Kenichi OHARA, Tomohito TAKUBO, Yasushi MAE, Tamio TANIKAWA, Tatsuo ARAI: "Design of a compact 3-DOF microhand system with large workspace," Proceedings of the 2011 International Symposium on Micro-Nano Mechatronics and Human Science, pp.63-68, 2011.

[11] James Nielsen, Tamio Tanikawa, and Tatsuo Arai:"Design and Analysis of a 3-DOF Micromanipulator," Proceedings of the 1999 IEEE International Conference on Robotics and Automation, pp.2183-2188, 1999.